Eigenmode analysis of superradiance

Jamal T. Manassah*
Department of Electrical Engineering, City College of New York, New York, New York 10031, USA
(Received 19 February 2014; published 12 May 2014)

Previous numerical work on the spatiotemporal distributions of the atomic polarization and of the difference in levels population of a one-dimensional system of two-level atoms initially inverted strongly suggested that the dynamics of the slab atomic ensemble in the linear regime of superradiance may best be treated by an eigenmode analysis. This method proved effective in obtaining both the time dependence of the atomic polarization and the spectral distribution of the emitted radiation from the slab in a number of physically interesting problems in the linear regime. In the present paper, I use the eigenfunction expansion technique to reduce the Maxwell-Bloch system of partial differential equations into a system of coupled first-order ordinary differential equations whose solutions clearly detail the contributions of the different modes to the system dynamics in the nonlinear regime of superradiant emission. I compute also the delay in time of the peak of the superradiant burst and its magnitude as functions of the ratio of the longitudinal decay rate to the transverse decay rate of the system.

DOI: 10.1103/PhysRevA.89.053815 PACS number(s): 42.50.Nn, 42.65.−k

I. INTRODUCTION

The seminal work of Dicke [1] on superradiance marked the beginning of the study of cooperative phenomena in a system of two-level atoms. A large number of theoretical publications on the shortening of the lifetime of the atomic system followed including the work of Rehler and Eberly [2], Bonifacio *et al.* [3], Sokolov and Trifonov [4], Bonifacio and Lugiato [5], Haake *et al.* [6,7], and others. Review papers and books that reported on the advances in the field include those of Gross and Haroche [8], Andreev *et al.* [9], Zheleznyakov *et al.* [10], and Benedict *et al.* [11]. More recently, a number of papers on superradiance in spin systems and magnets were as well published, including Chudnovsky and Garanin [12], Vanacken *et al.* [13], Benedict *et al.* [14], Yukalov and Yukolova [15], and others. Verification of superradiance was established in many experiments reported in papers by Skribano *et al.* [16], Gibbs *et al.* [17], Flusberg *et al.* [18], Florian *et al.* [19,20], Zinov'ev *et al.* [21], and others. The shortening of the atomic decay rate of the atomic system as compared to that of the isolated atom due to the presence of similar atoms, also referred to as cooperative decay rate (CDR), continues to be a subject of both theoretical and experimental interests.

Friedberg, Hartmann, and the author [22–24] extended the understanding of the cooperative quantum electrodynamics phenomenon beyond CDR. They predicted the existence of a parallel and simultaneous effect which they called the cooperative Lamb shift (CLS). This effect was observed experimentally only recently by the Roehlsberger group at DESY [25] and the C. S. Adams group at Durham [26].

Different mathematical tools were used in the theoretical analysis of superradiance; however, in a series of papers by the author and collaborators [27–29] investigating numerically the spatiotemporal dependence of the polarization in one-dimensional (1D) geometry during superradiance, it became clear that the eigenfunctions of the Liénard-Wiechert Green's function would be the mathematical functions best suited for analyzing the dynamics of this problem. These eigenfunctions, referred to as the "pressure induced cavity modes," were also independently discussed in [30,31]. It is within the context of the eigenfunction analysis that I consider the problem of superradiance here. This analysis was not carried out previously.

A key result of our early numerical calculations was that in the neighborhood of $u_0 = k_0 z_0 = (m + 1/4)\pi$ the dominant mode governing the dynamics of the system in the linear regime is always an even function, while for $u_0 = k_0 z_0 = (m - 1/4)\pi$, the dominant mode is an odd function, where m is an integer and $2z_0$ is the thickness of the slab. Only in very narrow strips centered at $u_0 = k_0 z_0 = m\pi$ or $u_0 = k_0 z_0 = (m - 1/2)\pi$, the spatial dependence of the polarization had no definite parity. In Fig. 1, I show the loci of the system eigenvalues in the complex plane for representative examples for each of the two well-defined parity families. As can be noted, the dominant mode (i.e., that with the largest real value) for $u_0 = 5\pi/4$ corresponds to an even mode, while that for $u_0 = 7\pi/4$ corresponds to an odd mode.

More recently [32,33] Friedberg and the author analyzed the mathematical structure of these eigenfunctions and derived the pseudo-orthogonality relation and the Parseval identity for these functions. This permitted the use of these functions in the analysis of many essentially linear problems of two-level atoms electrodynamics. Through the eigenfunction expansion technique, we calculated for the slab geometry (i) the dynamical Lorentz shift [34]; (ii) the pumping rate and the cw lasing frequency for a stationary state of N two-level atoms near threshold [35]; (iii) the spectral distribution of the emission from a slab prepared by a weak delta pulse [36], a problem initially suggested by Burnham and Chiao [37]; and (iv) the Purcell-Dicke effect [38], which predicts manyfold enhancement in the CDR of a collection of N two-level identical atoms between two metals when the plasmon frequency in the metal and that of the polariton in the two-level medium are in resonance. The eigenfunction method proved useful, as well, in solving many three-dimensional (3D) problems.

In this paper I show how the eigenfunction expansion can be used as well to analyze more transparently the nonlinear regime of emission. This method shows clearly the role of the

*Corresponding author: jmanassah@gmail.com

 ©2014 American Physical Society

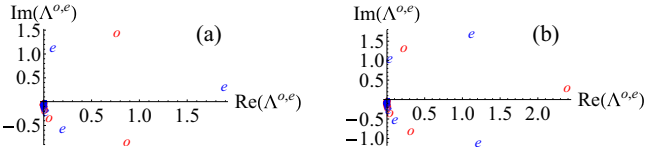

FIG. 1. (Color online) The values of the odd (o) and even (e) normalized eigenvalues for a slab of thickness $2z_0$. (a) $u_0 = k_0 z_0 = 5\pi/4$, (b) $u_0 = k_0 z_0 = 7\pi/4$.

different modes in the dynamics of the system. In particular, I show that the system of coupled Maxwell-Bloch equations, a nonlinear system of coupled partial differential equations, can be reduced to a system of coupled first-order nonlinear ordinary differential equations for the expansion coefficients of the dynamical variables in eigenfunctions.

Specifically, I compute the time dependence of the different expansion coefficients for two configurations, one where the dominant mode is an even function while in the other the dominant mode is an odd function. The onset of the nonlinearity is shown to follow the same structural patterns in both cases.

Furthermore, I compute the dependence of the normalized Rabi frequency maximum magnitude and its time delay at the exit plane of the slab as a function of the ratio of the longitudinal decay rate to the transverse decay rate of the system.

The paper is organized as follows: In Sec. II, the expressions for the Maxwell-Bloch equations in normalized coordinates are given; in Sec. III, the system of coupled ordinary differential equations describing the dynamics of the expansion coefficients are derived; in Sec. IV, the time-dependent solutions for the expansion coefficients are given; and in Sec. V, I make some concluding remarks.

II. MAXWELL-BLOCH EQUATIONS IN NORMALIZED COORDINATES

In this section, I summarize the form of the Maxwell-Bloch equations when written in normalized form.

Define the normalized variables for a slab of thickness $2\,z_0$ as

$$Z = z/z_0 \quad T = Ct \quad \Gamma_1 = \gamma_1/C \quad \Gamma_2 = \gamma_2/C \quad u_0 = k_0 z_0$$
$$\Omega_{c,0,L} = \omega_{c,0,L}/C,$$

where $\Omega_{c,0,L}$ are, respectively, the normalized electric field carrier frequency, the atomic transition frequency, and the Lorentz shift. In this system of units, all quantities are normalized to the parameter of interatomic cooperativity $C = \frac{4\pi N \wp^2}{\hbar V}$, where N is the number of particles, V is the slab volume, and $\wp$ is the reduced dipole moment of the atomic transition (its normalization is uniquely determined when given as a function of the isolated atom decay rate; see below). In these units, the transverse decay rate Γ_2, due to the instantaneous dipole-dipole interaction between atoms, is equal to 2.33/4, and the normalized Lorentz shift is equal to 1/3. The isolated atom decay rate $\gamma_1 = \frac{4}{3}\wp^2 k_0^3/\hbar$ specifies the longitudinal decay rate of the system.

The Maxwell-Bloch equations in 1D are given in these units by

$$\frac{\partial \chi(Z,T)}{\partial T} = -[i(\Omega_0 - \Omega_c) + \Gamma_T - i\Omega_L n(Z,T)]\chi(Z,T) + \frac{i}{2} n(Z,T)\psi(Z,T), \tag{1}$$

$$\frac{\partial n(Z,T)}{\partial T} = -i[\chi^*(Z,T)\psi(Z,T) - \chi(Z,T)\psi^*(Z,T)] + \Gamma_1(1 - n(Z,T)), \tag{2}$$

$$\psi(Z,T) = iu_0 \int_{-1}^{1} dZ' \chi(Z', T - \xi|Z - Z'|) \times \exp(iu_0|Z - Z'|), \tag{3}$$

where $\Gamma_T = \Gamma_2 + \Gamma_1/2$, χ (complex) and n (real) describe, respectively, the atomic polarization density and the degree of excitation of the two-level atoms ($n = 1$ if all atoms are in the ground state and $n = -1$ if all atoms are excited); ψ represents the normalized Rabi frequency of the complex electric field envelope; and $\xi = C\,z_0/c$, where c is the speed of light in vacuum.

The Markov approximation consists of neglecting the retardation effects in Eq. (3). This reduces to approximating Eq. (3) by

$$\psi(Z,T) = iu_0 \int_{-1}^{1} dZ' \chi(Z',T) \exp(iu_0|Z - Z'|). \tag{4}$$

In the following I shall consider cases where this approximation is valid.

III. EIGENFUNCTION DECOMPOSITION

I shall solve the system described by Eqs. (1), (2), (4) by expanding each of the quantities $\psi(Z,T)$, $n(Z,T)$, $\chi(Z,T)$ in the basis formed by the eigenfunctions of the integral equation:

$$\Lambda_s \varphi_s(Z) = \frac{u_0}{2} \int_{-1}^{1} dZ' \exp(iu_0|Z - Z'|)\varphi_s(Z'). \tag{5}$$

This integral equation admits two families of solutions, where the superscript refers, respectively, to (odd, even) parity in space, given, respectively, by

$$\varphi_s^o(Z) = \sin\left(v_s^o Z\right), \tag{6}$$

$$\varphi_s^e(Z) = \cos\left(v_s^e Z\right), \tag{7}$$

where the complex wave vectors (v_s^o, v_s^e) are solutions of the transcendental equations,

$$\cot\left(v_s^0\right) = i\,\frac{u_0}{v_s^o}, \tag{8}$$

$$\tan\left(v_s^e\right) = -i\,\frac{u_0}{v_s^e}, \tag{9}$$

where s, a positive integer, is the index of the solution.

These eigenfunctions form a complete set of basis functions for all functions over the interval $-1 \leqslant Z \leqslant 1$.

The eigenvalues associated with these eigenfunctions are given by

$$\Lambda_s^{o,e} = i\frac{u_0^2}{u_0^2 - \left(v_s^{o,e}\right)^2}. \tag{10}$$

Given that the kernel of Eq. (5) is non-Hermitian, its eigenfunctions do not obey the usual orthogonality relations of Hermitian operators (familiar from quantum mechanics); instead the eigenfunctions obey the following pseudo-orthogonal relations:

$$\int_{-1}^{1} \sin\left(v_s^o Z\right) \sin\left(v_{s'}^o Z\right) dZ = N_s^o \delta_{s,s'}, \tag{11}$$

where

$$N_s^o = 1 - \frac{\cos^2\left(v_s^o\right)}{iu_0}, \tag{12}$$

and

$$\int_{-1}^{1} \cos\left(v_s^e Z\right) \cos\left(v_{s'}^e Z\right) dZ = N_s^e \delta_{s,s'}, \tag{13}$$

where

$$N_s^e = 1 - \frac{\sin^2\left(v_s^e\right)}{iu_0}. \tag{14}$$

The Parseval identity for each of the above basis functions can be easily derived.

We decompose the dynamical variables in the eigenfunctions basis as

$$\psi(Z,T) = \sum_s e_s^o(T)\tilde{\varphi}_s^o(T) + \sum_s e_s^e(T)\tilde{\varphi}_s^e(T), \tag{15}$$

$$n(Z,T) = \sum_s \eta_s^o(T)\tilde{\varphi}_s^o(T) + \sum_s \eta_s^e(T)\tilde{\varphi}_s^e(T), \tag{16}$$

$$\chi(Z,T) = \sum_s p_s^o(T)\tilde{\varphi}_s^o(T) + \sum_s p_s^e(T)\tilde{\varphi}_s^e(T), \tag{17}$$

where the tilde over the eigenfunction is used to indicate that I am using the normalized eigenfunctions in the expansions.

From Eq. (5), one can directly deduce that

$$e_s^{o,e}(T) = i2\Lambda_s^{o,e} p_s^{o,e}(T). \tag{18}$$

Through a rotation of the polarization coefficients, the term $i(\Omega_c - \Omega_0)$ can be eliminated; I shall not, however, modify the notation used here for the rotated quantity but remember to measure frequency from the resonant frequency, if and when computing the spectral distribution. The coupled ordinary differential equations determining $p_s^{o,e}$ and $\eta_s^{o,e}$ can be directly obtained by combining Eqs. (1), (2), (15), (16), and (18) and using the pseudo-orthogonality conditions (11) and (13), to give the following set of ordinary differential equations in time:

$$\frac{dp_s^o(T)}{dT} = -\Gamma_T p_s^o(T) + \sum_m \sum_n A(s,m,n)\eta_m^o(T)p_n^e(T)\left[i\Omega_L - \Lambda_n^e\right] + \sum_m \sum_n B(s,m,n)\eta_m^e(T)p_n^o(T)\left[i\Omega_L - \Lambda_n^o\right], \tag{19}$$

$$\frac{dp_s^e(T)}{dT} = -\Gamma_T p_s^e(T) + \sum_m \sum_n C(s,m,n)\eta_m^o(T)p_n^o(T)\left[i\Omega_L - \Lambda_n^o\right] + \sum_m \sum_n D(s,m,n)\eta_m^e(T)p_n^e(T)\left[i\Omega_L - \Lambda_n^e\right], \tag{20}$$

$$\begin{aligned}\frac{d\eta_s^o(T)}{dT} = &-\Gamma_1 \eta_s^o(T) + 2\sum_m \sum_n \left[E_1(s,m,n)\bar{p}_m^o(T)\, p_n^e(T)\, \Lambda_n^e + E_2(s,m,n)p_m^o(T)\, \bar{p}_n^e(T)\, \bar{\Lambda}_n^e\right] \\ &+ 2\sum_m \sum_n \left[F_1(s,m,n)\bar{p}_m^e(T)\, p_n^o(T)\, \Lambda_n^o + F_2(s,m,n)p_m^e(T)\, \bar{p}_n^o(T)\, \bar{\Lambda}_n^o\right],\end{aligned} \tag{21}$$

$$\begin{aligned}\frac{d\eta_s^e(T)}{dT} = &-\Gamma_1 \eta_s^e(T) + \Gamma_1 I_s^e + 2\sum_m \sum_n \left[G_1(s,m,n)\bar{p}_m^o(T)\, p_n^o(T)\, \Lambda_n^o + G_2(s,m,n)\bar{p}_m^e(T)\, p_n^e(T)\, \Lambda_n^e\right] \\ &+ 2\sum_m \sum_n \left[H_1(s,m,n)p_m^o(T)\, \bar{p}_n^o(T)\, \bar{\Lambda}_n^o + H_2(s,m,n)p_m^e(T)\, \bar{p}_n^e(T)\, \bar{\Lambda}_n^e\right],\end{aligned} \tag{22}$$

where

$$\tilde{\varphi}_m^0(Z) = \frac{1}{\sqrt{N_m^0}} \sin\left(v_m^0 Z\right), \tag{23a}$$

$$\tilde{\varphi}_m^e(Z) = \frac{1}{\sqrt{N_m^e}} \cos\left(v_m^e Z\right), \tag{23b}$$

$$I_s^e = \int_{-1}^{1} dZ\tilde{\varphi}_s^e(Z) = \frac{2}{\sqrt{N_s^e}} \frac{\sin\left(v_s^e\right)}{v_s^e}, \tag{24}$$

$$A(s,m,n) = \int_{-1}^{1} dZ\tilde{\varphi}_s^o(Z)\tilde{\varphi}_m^o(Z)\,\tilde{\varphi}_n^e(Z), \tag{25}$$

$$B(s,m,n) = \int_{-1}^{1} dZ\tilde{\varphi}_s^o(Z)\tilde{\varphi}_m^e(Z)\,\tilde{\varphi}_n^o(Z) = A(s,n,m), \tag{26}$$

$$C(s,m,n) = \int_{-1}^{1} dZ\tilde{\varphi}_s^e(Z)\tilde{\varphi}_m^o(Z)\,\tilde{\varphi}_n^o(Z) = A(n,m,s), \tag{27}$$

$$D(s,m,n) = \int_{-1}^{1} dZ\tilde{\varphi}_s^e(Z)\tilde{\varphi}_m^e(Z)\,\tilde{\varphi}_n^e(Z), \tag{28}$$

$$E_1(s,m,n) = \int_{-1}^{1} dZ\tilde{\phi}_s^o(Z)\bar{\tilde{\phi}}_m^o(Z)\,\tilde{\phi}_n^e(Z), \tag{29}$$

$$E_2(s,m,n) = \int_{-1}^{1} dZ \tilde{\phi}_s^o(Z)\tilde{\phi}_m^o(Z)\bar{\tilde{\phi}}_n^e(Z), \tag{30}$$

$$F_1(s,m,n) = \int_{-1}^{1} dZ \tilde{\phi}_s^o(Z)\bar{\tilde{\phi}}_m^e(Z)\tilde{\phi}_n^o(Z) = E_2(s,n,m), \tag{31}$$

$$F_2(s,m,n) = \int_{-1}^{1} dZ \tilde{\varphi}_s^o(Z)\tilde{\varphi}_m^e(Z)\bar{\tilde{\varphi}}_n^o(Z) = E_1(s,n,m), \tag{32}$$

$$G_1(s,m,n) = \int_{-1}^{1} dZ \tilde{\phi}_s^e(Z)\bar{\tilde{\phi}}_m^o(Z)\tilde{\phi}_n^o(Z) = E_1(n,m,s), \tag{33}$$

$$G_2(s,m,n) = \int_{-1}^{1} dZ \tilde{\varphi}_s^e(Z)\bar{\tilde{\varphi}}_m^e(Z)\tilde{\varphi}_n^e(Z), \tag{34}$$

$$H_1(s,m,n) = \int_{-1}^{1} dZ \tilde{\phi}_s^e(Z)\tilde{\phi}_m^o(Z)\bar{\tilde{\phi}}_n^o(Z) = E_1(m,n,s), \tag{35}$$

$$H_2(s,m,n) = \int_{-1}^{1} dZ \tilde{\phi}_s^e(Z)\tilde{\phi}_m^e(Z)\bar{\tilde{\phi}}_n^e(Z) = G_2(s,n,m). \tag{36}$$

As noted above, of the 12 overlap integrals only five are independent. The closed form expressions for the five primitive overlap integrals (A,D,E_1,E_2,G_2) can be easily obtained using the standard techniques for the product of three sine or cosine functions; for example,

$$A(s,m,n) = \frac{1}{2\sqrt{N_s^o N_m^o N_n^e}}\left[-\frac{\sin\left(v_n^e - v_m^0 - v_s^o\right)}{v_n^e - v_m^0 - v_s^o} + \frac{\sin\left(v_n^e + v_m^0 - v_s^o\right)}{v_n^e + v_m^0 - v_s^o} + \frac{\sin\left(v_n^e - v_m^0 + v_s^o\right)}{v_n^e - v_m^0 + v_s^o} - \frac{\sin\left(v_n^e + v_m^0 + v_s^o\right)}{v_n^e + v_m^0 + v_s^o}\right]. \tag{25a}$$

In the next section, I shall report the results for solving the system of Eqs. (19)–(22) for the slab having $u_0 = 5\pi/4$ and the slab having $u_0 = 7\pi/4$ (the first having an even mode as the dominant mode, while an odd mode is the dominant mode in the second case). I shall include in the computation, for each case a total of 40 modes (20 even modes and 20 odd modes). The initial value for each of the $p_m^{o,e}$ is chosen to be equal to 10^{-4}. This ensures that the normalized Rabi frequency at the exit plane is equal, at $T = 0$, to the square root of the mean square electric field resulting from the quantum fluctuations. At the end of the next section, I shall also investigate the effects of introducing a random phase in the values of the initial conditions to model the conditions of complete incoherence in the polarization at initial time.

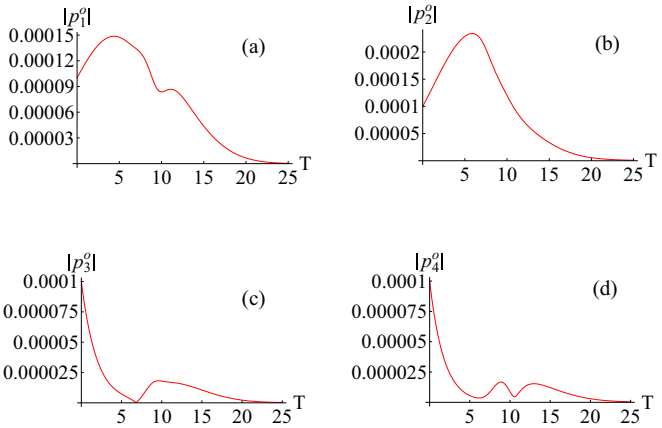

FIG. 2. (Color online) The magnitude of the odd coefficients of the eigenfunctions expansion of the polarization are plotted as a function of the normalized time for a system initially inverted. $u_0 = k_0 z_0 = 5\pi/4$, $\frac{\Gamma_1}{\Gamma_2} = 0.05$. (a) $m = 1$, (b) $m = 2$, (c) $m = 3$, (d) $m = 4$.

IV. RESULTS

Combining Eq. (18) with Eq. (1), one notes that in the linear regime of superradiance, i.e., $n \cong -1$, the time development of $p_s^{o,e}(T)$ is given by the ordinary differential equation (ODE):

$$\frac{dp_s^{o,e}(T)}{dT} \cong -\left[i\Omega_L + \Gamma_T - \Lambda_s^{o,e}\right] p_s^{o,e}. \tag{37}$$

This implies that each of the polarization components grows initially at the rate equal to $\mathrm{Re}(\Lambda_s^{o,e}) - \Gamma_T$. This confirms the known results [27–29] that in the linear regime of superradiance, the polarization spatial distribution is approximately given by that of the dominant eigenmode [that with the largest value of $\mathrm{Re}(\Lambda_s^{o,e})$], when only one of these exists.

It is further noted that the coefficients of all modes with $\mathrm{Re}(\Lambda_s^{o,e}) < \Gamma_T$ damp out initially. An examination of Figs. 2 and 3, pertaining to the case $u_0 = 5\pi/4$ at small T verifies

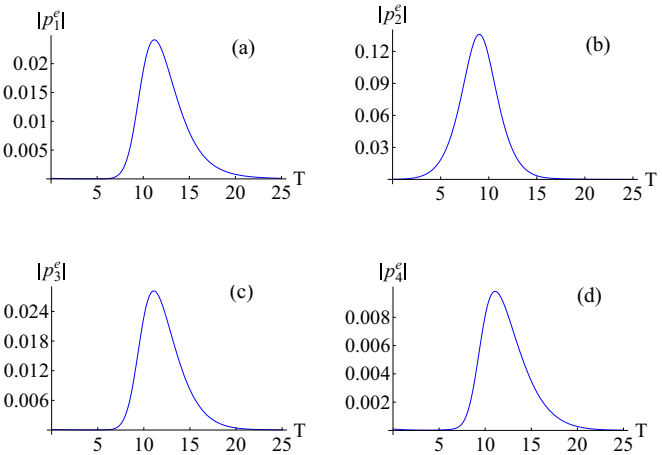

FIG. 3. (Color online) The magnitude of the even coefficients of the eigenfunctions' expansion of the polarization are plotted as a function of the normalized time for a two-level system initially inverted. $u_0 = k_0 z_0 = 5\pi/4$, $\frac{\Gamma_1}{\Gamma_2} = 0.05$. (a) $m = 1$, (b) $m = 2$, (c) $m = 3$, (d) $m = 4$.

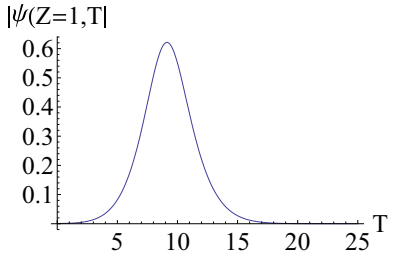

FIG. 4. (Color online) The normalized Rabi frequency at the outgoing plane is plotted as a function of the normalized time for a two-level system initially inverted. $u_0 = k_0 z_0 = 5\pi/4$, $\frac{\Gamma_1}{\Gamma_2} = 0.05$.

the above results. Having established the small T behavior for each of the expansion coefficients, I note the general pattern observed at later times: Essentially, the dominant mode and other leading modes, of the same parity, increase successively to different maximum values, then decay. One notes that the dominant mode maximum value is larger than any of the other maxima and occurs at an earlier time than that of the others: The values of the magnitude of the maxima of the different expansion coefficients and their time delay for the dominant and leading modes (all even) are given, respectively, by the following $(m, |p_m^e(T_m^{\max})|, T_m^{\max})$: (2, 0.135, 9.034), (3, 0.028, 11.09), (1, 0.024, 11.22), (4, 0.0096, 11.07).

The value of the normalized Rabi frequency as a function of time at the outgoing plane can be obtained by combining Eqs. (15) and (18). It is given by

$$\psi(Z=1,T) = 2i\left[\sum_m \Lambda_m^e p_m^e(T)\frac{\cos\left(v_m^e\right)}{\sqrt{N_m^e}} + \sum_m \Lambda_m^o p_m^o(T)\frac{\sin\left(v_m^o\right)}{\sqrt{N_m^o}}\right]. \tag{38}$$

The magnitude of this quantity is plotted as a function of the normalized time in Fig. 4.

The values of the maximum of this curve and its location are given for $u_0 = 5\pi/4$ by $\psi(Z=1,T^{\max}) = 0.621$, $T^{\max} = 9.129$.

In Fig. 5, I plot the magnitude of the polarization as a function of the normalized distance inside the slab at $T^{\max} - 2$ and at $T^{\max}$. (The peak of the superradiant burst is at $T^{\max}$.)

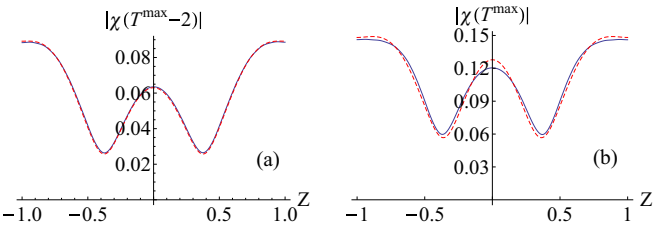

FIG. 5. (Color online) The magnitude of the normalized polarization is plotted as a function of the normalized distance for a two-level system initially inverted. $u_0 = k_0 z_0 = \frac{5\pi}{4}$, $\frac{\Gamma_1}{\Gamma_2} = 0.05$ (a) at $T = T^{\max} - 2$, (b) at $T = T^{\max}$. Solid curve: contribution from all 40 modes are included; dashed curve: contribution from the even $m = 1,2,3$ are only included.

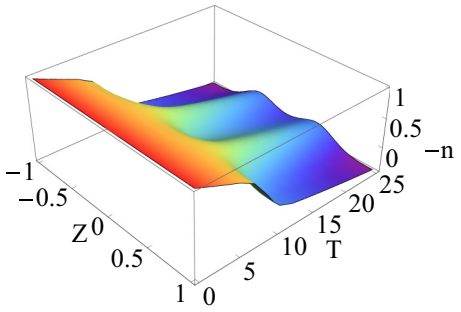

FIG. 6. (Color online) The negative of the population difference is plotted as a function of the normalized time and normalized distance for a two-level system initially inverted. $u_0 = k_0 z_0 = 5\pi/4$, $\frac{\Gamma_1}{\Gamma_2} = 0.05$.

One notes that in the linear regime of superradiance, this curve is uniquely determined by the dominant mode, while at $T^{\max}$, it takes the contribution from the dominant mode and the leading modes to reproduce the polarization spatial profile.

In Fig. 6, I plot the spatiotemporal distribution of the difference of population. One notes that the upper state population starts depleting shortly before $T^{\max}$, thus validating the results shown in Fig. 5, showing that the system is already well in the nonlinear regime at the superradiant burst peak.

In order to validate the general features observed in Figs. 2–6, I recompute and plot in Figs. 7–11 for the slab with $u_o = 7\pi/4$ the same quantities as in Figs. 2–6 for the slab with $u_o = 5\pi/4$. In this case, the dominant mode is odd.

One notes that all the general patterns for the onset and buildup of the superradiant burst, previously observed, are reproduced in this case as well. The respective $(m, |p_m^o(T_m^{\max})|, T_m^{\max})$ for the dominant and leading modes (all odd) are (2, 0.2097, 5.764), (3, 0.0797, 6.953), (1, 0.0825, 7.083), (4, 0.0212, 8.079). In this instance $\psi(Z=1,T^{\max}) = 1.426$, $T^{\max} = 5.857$.

In Fig. 12, I plot the dependence of the magnitude of the peak of the normalized Rabi frequency at the exit plane and its location as a function of the ratio of the longitudinal decay rate to the transverse decay rate. One obtains the physically

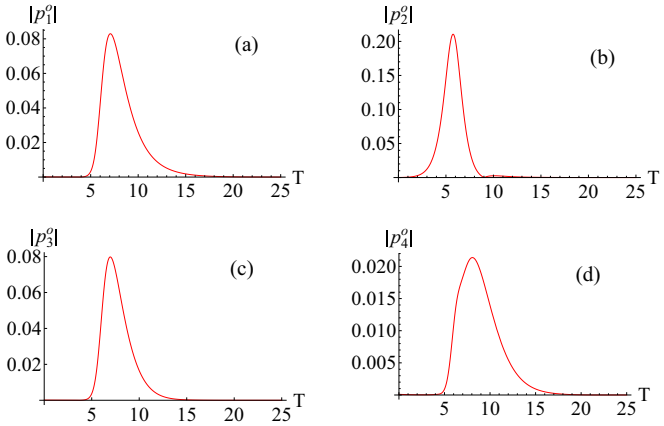

FIG. 7. (Color online) Same as Fig. 2 except that $u_0 = k_0 z_0 = 7\pi/4$.

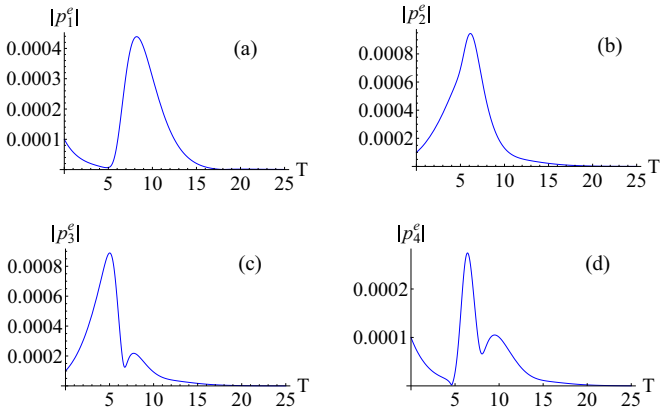

FIG. 8. (Color online) Same as Fig. 3 except that $u_0 = k_0 z_0 = 7\pi/4$.

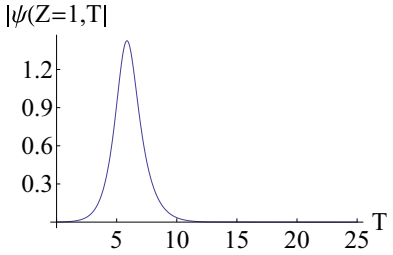

FIG. 9. (Color online) Same as Fig. 4 except that $u_0 = k_0 z_0 = 7\pi/4$.

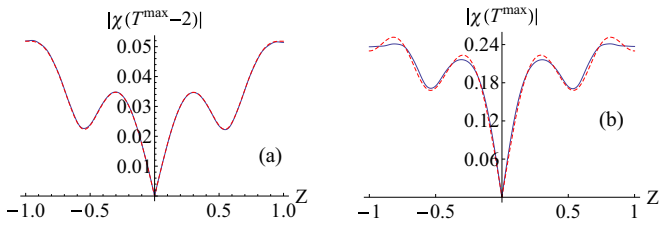

FIG. 10. (Color online) The magnitude of the normalized polarization is plotted as a function of the normalized distance for a two-level system initially inverted. $u_0 = k_0 z_0 = 7\pi/4$, $\frac{\Gamma_1}{\Gamma_2} = 0.05$ (a) at $T = T^{\max} - 2$, (b) at $T = T^{\max}$. Solid curve: contribution from all 40 modes are included; dashed curve: contribution from the odd $m = 1,2,3,4,5,6$ are only included.

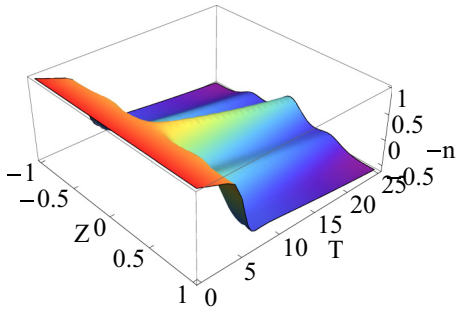

FIG. 11. (Color online) Same as Fig. 6 except that $u_0 = k_0 z_0 = 7\pi/4$.

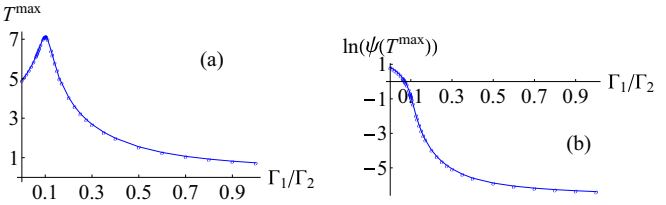

FIG. 12. (Color online) (a) The position and (b) the height of the maximum of the normalized Rabi frequency at the outgoing plane of a slab, for an initially inverted two-level system, are plotted as a function of the ratio Γ_1/Γ_2, $u_0 = k_0 z_0 = 7\pi/4$.

intuitive result that the peak of the burst decreases very fast with an increase of this ratio; however, these results show that the location (delay in time) of this peak initially increases, before decreasing.

Last, I examine the effect of including a random phase in the expressions for the initial values of $p_m^{o,s}(T = 0)$. This modification is intended to bring the semiclassical Maxwell-Bloch system of equations in closer agreement with the full quantum theory.

If I choose for each of the even and odd eigenfunction families a random phase from the interval $[0,2\pi]$ the values obtained for the magnitude and location of the peaks of the curves plotting $|p_m^o(T)|$ as a function of normalized time for the odd modes having $m = 1\cdots4$ are, respectively, (0.0825, 7.083), (0.2097, 5.764), (0.0798, 6.953), (0.0212, 8.078).

Comparing these values with the corresponding values with no initial random phase, one notes that corresponding quantities differ everywhere by much less than 1%. This provides an estimate of the error that one should expect in computing the features of the superradiant burst in treating this problem through the semiclassical Maxwell-Bloch equations.

V. CONCLUDING REMARKS

In this paper, a mathematical technique for analyzing and computing solutions of the Maxwell-Bloch equations in the nonlinear regime is detailed. This method is applied to the problem of superradiance.

Specifically, I showed the following:

(1) The problem of the electrodynamics of a two-level atom system can be analyzed transparently in the nonlinear regime through the use of the 1D Wiechert-Liénard Green's function eigenfunctions expansion; in particular, it is now possible to follow the dynamics of each mode through the different phases of the superradiant emission.

(2) The main dynamical features leading to the mixing of the different modes in the nonlinear regime of superradiance follow the same general patterns for slabs of different thicknesses.

(3) The peak magnitude of the superradiant burst decreases as the value of the ratio of the longitudinal decay rate over the transverse decay rate increases; the delay in the temporal position of this peak initially increases before decreasing. These results provide specific guidelines for the density of atoms needed to experimentally observe superradiance.

Last, I note that the technical limitation associated with analyzing the nonlinear problems through the method of

eigenfunctions is the issue of memory management in the numerical computation. The dimensions of each of the overlap integrals tensor are $(l \times l \times l)$ where $l \geqslant 5u_0$, if an accuracy of less than 1% error in the results is desired.

ACKNOWLEDGMENT

This work extends further a research program that Richard Friedberg and I jointly initiated on the quantum electrodynamics of an ensemble of two-level atoms.

[1] R. Dicke, Phys. Rev. **93**, 99 (1954).
[2] N. E. Rehler and J. H. Eberly, Phys. Rev. A **3**, 1735 (1971).
[3] K. Bonifacio, P. Schwendimann, and F. Haake, Phys. Rev. A **4**, 302 (1971); **4**, 854 (1971).
[4] I. V. Sokolov and E. D. Trifonov, Zh. Eksp. Teor. Fiz. **65**, 74 (1974).
[5] R. Bonifacio and L. A. Lugiato, Phys. Rev. A **11**, 1507 (1975); **12**, 587 (1975).
[6] F. Haake, H. King, G. Schroder, J. Haus, and R. Glauber, Phys. Rev. A **20**, 2047 (1979).
[7] F. Haake, J. W. Haus, H. King, G. Schroder, and R. Glauber, Phys. Rev. A **23**, 1322 (1981).
[8] M. Gross and S. Haroche, Phys. Rep. **93**, 301 (1982).
[9] A. V. Andreev, V. I. Emel'yanov, and Yu. A. Il'inskii, *Cooperative Effects in Optics* (Institute of Physics Publishing Ltd, Bristol, England, 1993).
[10] V. V. Zheleznyakov, V. V. Kocharovskii, and Vl. V. Kocharovskii, Usp. Fiz. Nauk **159**, 193 (1989).
[11] M. G. Benedict, A. M. Ermolaev, V. A. Malyshev, I. V. Sokolov, and E. D. Trifonov, *Superradiance: Multiatomic Coherent Emission* (Institute of Physics Publishing Ltd, Bristol, England, 1996).
[12] E. M. Chudnovsky and D. A. Garanin, Phys. Rev. Lett. **89**, 157201 (2002).
[13] J. Vanacken, S. Stroobants, M. Malfait, and V. V. Moshchalkov, M. Jordi, J. Tejada, R. Amigo, E. M. Chudnovsky, and D. A. Garanin, Phys. Rev. B **70**, 220401 (2004).
[14] M. G. Benedict, P. Foldi, and F. M. Peeters, Phys. Rev. B **72**, 214430 (2005).
[15] V. I. Yukalov and E. P. Yukalova, Laser Phys. Lett. **8**, 804 (2011).
[16] N. Skribano, I. P. Herman, J. C. MacGilli, and M. S. Feld, Phys. Rev. Lett. **30**, 309 (1973).
[17] H. M. Gibbs, Q. H. F. Vrehen, and H. M. J. Hikspoors, Phys. Rev. Lett. **39**, 547 (1977).
[18] A. Flusberg, T. Mossberg, and S. R. Hartman, Phys. Lett. **58**, 373 (1976).
[19] R. Florian, L. O. Schwan, and D. Schmid, Solid State Commun. **42**, 55 (1982).
[20] R. Florian, L. O. Schwan, and D. Schmid, Phys. Rev. A **29**, 2709 (1984).
[21] P. V. Zinovev, S. V. Lopina, Yu. V. Naboikin *et al.*, Zh. Eksp. Teor. Fiz. **85**, 1945 (1983).
[22] R. Friedberg, S. R. Hartmann, and J. T. Manassah, Phys. Rep. **7**, 101 (1973).
[23] J. T. Manassah, Phys. Rep. **101**, 359 (1983).
[24] J. T. Manassah, Adv. Opt. Photon. **4**, 108 (2012).
[25] R. Roehlsberger, K. Schlage, B. Sahoo, S. Couet, and R. Ruffer, Science **328**, 1248 (2010).
[26] J. Keaveney, A. Sargsyan, U. Krohn, I. G. Hughes, D. Sarkisyan, and C. S. Adams, Phys. Rev. Lett. **108**, 173601 (2012).
[27] J. T. Manassah and B. Gross, Opt. Commun. **143**, 329 (1997).
[28] J. T. Manassah and I. Gladkova, Opt. Commun. **189**, 87 (2001).
[29] J. T. Manassah and I. Gladkova, Opt. Commun. **196**, 221 (2001).
[30] S. Prasad and R. J. Glauber, Phys. Rev. A **61**, 063814 (2000).
[31] H. E. Tureci, A. D. Stone, and L. Ge, Phys. Rev. A **76**, 013813 (2007).
[32] R. Friedberg and J. T. Manassah, Phys. Lett. A **372**, 4164 (2008).
[33] R. Friedberg and J. T. Manassah, Phys. Lett. A **372**, 5131 (2008).
[34] R. Friedberg and J. T. Manassah, Phys. Lett. A **373**, 3423 (2009).
[35] R. Friedberg and J. T. Manassah, Phys. Lett. A **374**, 3389 (2010).
[36] J. T. Manassah, Laser Phys. **22**, 559 (2012).
[37] D. C. Burnham and R. Y. Chiao, Phys. Rev. **188**, 667 (1969).
[38] J. T. Manassah, Phys. Rev. A **88**, 053805 (2013).